ENTE PER LE NUOVE TECNOLOGIE,
L'ENERGIA E L'AMBIENTE

ISSN/0393-3016

Tb^{3+}-DOPED SILICATE GLASSES ENRICHED WITH BORON AND BARIUM FOR THE DETECTION OF NEUTRONS AND HIGH POWER X-RAYS

S. BACCARO, A. CECILIA, R. ROSA, A. VENEZIA

ENEA - Unità Tecnico Scientifica Tecnologie Fisiche Avanzate
Centro Ricerche Casaccia, Roma

LUCA NENCINI

ENEA - Biotecnologie, Protezione della Salute e degli Ecosistemi
Centro Ricerche Casaccia, Roma

P. FABENI, G.P. PAZZI

IFAC "N. Carrara" del CNR, Firenze

RT/2003/32/FIS

This report has been prepared and distributed by: Servizio Edizioni Scientifiche - ENEA Centro Ricerche Frascati, C.P. 65 - 00044 Frascati, Rome, Italy

Tb^{3+}-DOPED SILICATE GLASSES ENRICHED WITH BORON AND BARIUM FOR THE DETECTION OF NEUTRONS AND HIGH POWER X-RAYS

S. BACCARO, A. CECILIA, R. ROSA, A. VENEZIA, L. NENCINI, P. FABENI, G.P. PAZZI

Abstract

In this work, we studied a set of barium-rich and boron-rich silicate glasses, which are suitable to detect high power X-rays and neutrons, respectively. The former samples underwent a complete optical characterisation, including radiation damage, transmission spectra, decay kinetics and emission spectra. Irradiation tests were performed at the ^{60}Co "Calliope" radioisotope source (Enea-Casaccia, Rome) and the photoluminescence emission spectra and decay kinetics were studied using a XeCl excimer laser with λ_{exc}=308 nm (IFAC-CNR, Florence). The boron-enriched glasses were submitted to neutron radiography measurements, performed at the TRIGA thermal reactor (Enea-Casaccia, Rome). Analysed parameters turned out to be strongly dependent on glass composition and the influence of the main glass constituents is discussed as well.

Keywords: *Scintillator, Luminescence, Activator, Glassy Matrix, Radiation Hardness, Neutron Radiography.*

Riassunto

In questo lavoro sono stati analizzati dei silicati arricchiti con bario e con boro che trovano utilizzo rispettivamente nel campo della rivelazione dei raggi X di alta potenza e nella rivelazione dei neutroni. I primi sono stati sottoposti ad una caratterizzazione ottica completa, comprensiva del danno da radiazione, trasmissione ottica, cinetica di decadimento e spettri di emissione. Le prove di irraggiamento sono state effettuate presso la sorgente radioisotopica di ^{60}Co "Calliope" (CR Enea-Casaccia, Roma) e gli spettri di emissione e la cinetica di decadimento sono stati studiati presso l'IFAC-CNR (Firenze) utilizzando un laser ad eccimeri (λ_{exc}=308 nm). I vetri arricchiti con boro sono stati sottoposti a misure di radiografia neutronica, effettuate presso il reattore nucleare termico TRIGA (CR Enea-Casaccia, Roma). I risultati ottenuti hanno mostrato che i parametri investigati dipendono fortemente dalla composizione dei vetri.

Parole chiave: Scintillatori, Luminescenza, Attivatore, Matrice vetrosa, danno da radiazione, radiografia neutronica.

Index

Introduction

In many applications, an interesting alternative to scintillating crystals is represented by glassy matrices, opportunely activated and characterised by good chemical and mechanical stabilities. Glass matrices offer several advantages with respect to crystals, as easy shaping of elements, excellent chemical durability and thermal shock resistance. Glasses are also characterised by low production cost techniques, such as moulding, hot pressing and extrusion and possibility to be adjusted in composition in a comparatively large range to meet the requirements of the various applications. The only problem related to the use of glassy scintillators with respect to crystals is their low light production related to a low energy transfer efficiency from the matrix to the luminescent centres. Such behaviour is due to the presence of many trapping sites in the structure where charge carries can be entrapped giving rise to non-radiative recombination processes. In this sense glassy scintillators could become really competitive with crystals only if their light production will be reinforced. A possibility that can be adopted to increase the scintillation efficiency is the glass co-doping with some specific ions that act as mediators between the glass matrix and the luminescent centres. Rare earth ions are frequently used to optically activate glass matrices, among which Ce^{3+}, Tb^{3+}, Eu^{3+} and Pr^{3+} are often adopted [1, 2]. These ions are characterised by different emission spectra and decay kinetics that make them suitable for different applications. Ce^{3+} ion emits light in the ultraviolet spectral region while Pr^{3+} scintillates in the red and near infrared spectral regions and weakly in the blue around 485 nm. The emission spectrum of Tb^{3+} consists of four leading lines at 482 nm, 542.5 nm, 585 nm and 621 nm belonging to the Tb^{3+} electronic transitions $^5D_4 \rightarrow {}^7F_X$ (X=6, 5, 4, 3 respectively). Eu^{3+} luminescence spectrum consists of two bands centred around 591 nm and 613 nm. The first peak is due to the $^5D_0 \rightarrow {}^7F_1$ transition and the second (the dominating one) is due to the $^5D_0 \rightarrow {}^7F_2$ transition. From the kinetic point of view, they all give rise to a fast response with typical decay times of about 20-50 ns (Ce^{3+}) and few ns (Pr^{3+}, Eu^{3+}). On the contrary, Tb^{3+} ions are characterised by a spectrum with a much slower decay time of 3.0 ms in silicate glasses [1].

In this work, we studied two kinds of Tb^{3+}-containing silicate glasses enriched with barium and boron. The former glasses can be used to detect high power X-rays because of the barium high X-ray attenuation coefficient; as far as the boron enriched glasses are concerned, they can be used to detect thermal neutrons thanks to the boron interaction cross section with neutrons.

The barium containing glasses underwent a complete optical characterisation, including radiation damage, transmission spectra, decay kinetics and emission spectra. Irradiation tests were performed at the ^{60}Co "Calliope" radioisotope source (Enea-Casaccia, Rome) and the photoluminescence emission spectra and decay kinetics were studied using a XeCl excimer laser with λ_{exc}=308 nm (IFAC-CNR, Florence). The boron-enriched glasses were tested at the TRIGA thermal reactor (Enea-Casaccia, Rome) where an experimental set-up is available to perform neutron radiography measurements.

CHAPTER 1: SAMPLES AND EXPERIMENTAL SET-UP

1.1 Sample composition

The analysed glasses were produced at the "Vavilov" State Optical Institute of Saint Petersburg (Russia) and they are characterised by the composition reported in Table I. The TK2, TK8, TK12 and TK13 samples are the barium rich glasses while the BK10 and BK11 samples are doped with boron.

Table I: Sample composition

Activators and Properties	TK12	TK2	TK13	TK8	BK10	BK11
Tb_2O_3 *mol.%*	2.7	2.1	4.2	4.2	4.2	4.2
Gd_2O_3 *mol.%*	-	0.8	-	-	-	-
CeO_2 *mol.%*	-	-	-	0.5	-	-
Density *(g/cm^3)*	4.1	4.1	4.3	4.3	4.5	4.5
Dimension *(mm^3)*	20x20x10	20x20x10	20x20x10	20x20x8	30x30x1.5	30x30x0.3

1.2 Facilities

1.2.a "Calliope" γ facility

"Calliope" γ plant is a pool-type irradiation facility equipped with a ^{60}Co radioisotope source placed in a high-volume (7x6x3.9 m^3) and shielded cell [3]. The source is characterised by a cylindrical geometry with the ^{60}Co pencils placed in the rack circumference (Figure 1). The emitted radiation consists of two γ photons with energy of 1.17 MeV and 1.33 MeV, mean energy being 1.25 MeV. The maximum licensed activity is $3.7 \cdot 10^{15}$ Bq and the present activity is $9.05 \cdot 10^{14}$ Bq (January 1, 2003). This plant offers the possibility to choose the dose rate for sample irradiation and the maximum dose rate (along the rack longitudinal axis) is 8240 Gy/h (January 1, 2003). The storage water pool dimensions are 2x4.5x8 m^3 and two separate source emergency storage wells are positioned on the bottom of the pool. The irradiation protection shield is realized in baritic concrete (180 cm thickness).

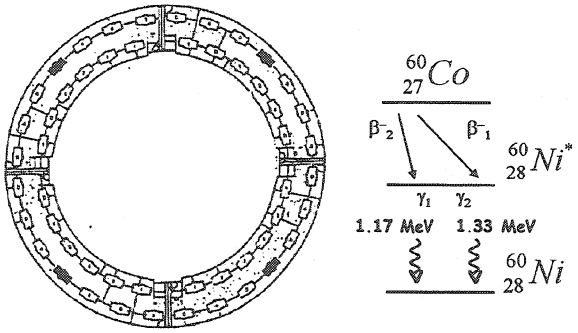

Figure 1: "Calliope" rack circumference and ^{60}Co decay.

To determine the irradiation dose rate, at the "Calliope plant" three different dosimetric methods are available [4]: the Fricke absolute dosimetry (20-400 Gy), the alanine dosimetry (from few Gy up to 500 kGy) and the Red Perspex dosimetry (5-50 kGy). Each irradiation test is performed in charge particle equilibrium conditions and according to the various user demands (as the possibility to perform temperature controlled tests).

1.2.b TRIGA reactor

TRIGA RC-1 is a pool thermal reactor with a horizontal section reported in Figure 2. Its core is placed in a cylindrical graphite reflector, on an aluminium vessel [3]. The vessel is filled with demineralised water that has the function of moderator, coolant and biological shield. The fuel consists of cylindrical elements formed by a ternary alloy of Zr-H and 20% enriched uranium ^{235}U (total mass around 4,5 kg of ^{235}U). Therefore moderation is assured not only by cooling water but also by an alloy of zirconium hydride, which is also responsible for the prompt high negative temperature coefficient. The reactor is controlled by four rods: 2 shims, 1 safety and 1 regulating rod.

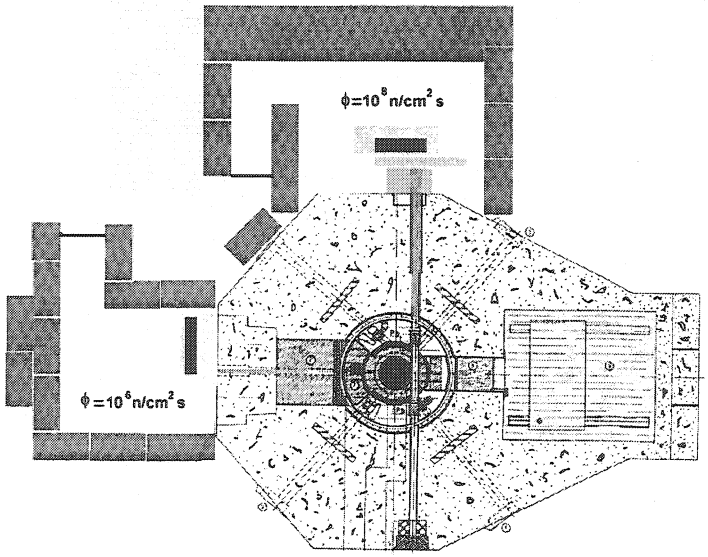

Figure 2: TRIGA RC-1 horizontal section.

An Am-Be source provides the controlled and gradual initiation of the chain reaction. The heat produced by the core is removed by natural water circulation. Water of cooling system is kept at constant temperature by a suitable circuit provided with a heat

exchanger and cooling towers. TRIGA maximum exercise power is 1 MW, the highest neutron thermal flux is $3*10^{13}$ n/cm^{2}s (central thimble) and the highest γ dose rate is 1.03 MGy/h (central thimble).

1.3 Optical Measurements

1.3.a Transmission

Transmission measurements were performed in the UV-visible spectral region (200-800 nm) by using both a commercial Perkin Elmer spectrophotometer and a home made double-ray spectrophotometer. The first instrument is suitable to measure short and parallel surface sample while the second instrument allows to investigate also diffusive and not perfectly shaped crystals, thanks to the integrating sphere by which the transmitted light is collected. To evaluate the distribution of colour centres induced by ionising irradiation the so-called radiation induced absorption coefficient is used, given by the following formula:

$$\mu = \frac{1}{L} \cdot \ln\left(\frac{T_0}{T}\right) \qquad (1.1)$$

where T and T_0 are the transmissions before and after irradiation, and L is the sample length (m). After each irradiation, glasses were annealed in air atmosphere at a temperature of 330 °C (10 hours) in order to restore their initial optical conditions.

1.3.b UV Luminescence

Luminescence measurements were performed by a Perkin Elmer spectrofluorimeter (MPF). Glass samples were excited at λ_{exc}=380 nm and the emission spectra were studied between 420 and 700 nm. The specrofluorimeter response function has been evaluated measuring the emission of a calibrated black body radiation source (Oriel lamp, 3000 K). All spectra were corrected for this response function:

$$S(\lambda) = \frac{I(\lambda)}{L(\lambda)} \qquad (1.2)$$

where $L(\lambda)$ is the detector quantum efficiency given by the producer (Oriel) and $I(\lambda)$ is the lamp emission spectrum.

1.3.c Decay Time

The emission decay kinetics of a scintillator can be approximated by a multiexponential expression:

$$I(t) = \sum_i A_i * e^{-\frac{t}{\tau_i}} \qquad (1.3)$$

where τ_i is the decay time and A_i the signal intensity. Photoluminescence and decay kinetics measurements were performed at the IFAC-CNR Institute (Florence). The experimental set-up is reported in Figure 3 and it is based on a XeCl excimer laser source (Mod. ML 780U). The gas mixture consists of Xe (40 mbar), HCl (80 mbar) and He (total pressure of 1,9 bar). The frequency of discharge is 10-20 Hz and the pulse duration is around 10-12 ns, energy up to 10 mJ. Between the laser and the sample, there are two beam splitters (BS) followed by two photomultipliers; the former is used as a trigger for the oscilloscope, the latter is the reference signal of the laser, in order to monitor the excitation laser intensity for each measurement. The emission is observed at 90° by a PC driven spectrometer Jobin-Yvon (triax 320) two channels: in the former

channel, a fast photomultiplier (arise time of 2 ns) allows to collect the emission decay curve analysed by a digital sampling oscilloscope (Tektronix TDS 680D) giving time decays on a temporal scale ranging from ns to s and amplitudes varying in six orders of magnitude. In the latter channel, an Optical Multichannel Analyzer (OMA) EG&G PARC 1461 with a linear photodiode array allows to obtain emission spectra between 250-800 nm, in continuous way (CW) or in time resolved way (TR, with windows of 20 ns or greater).

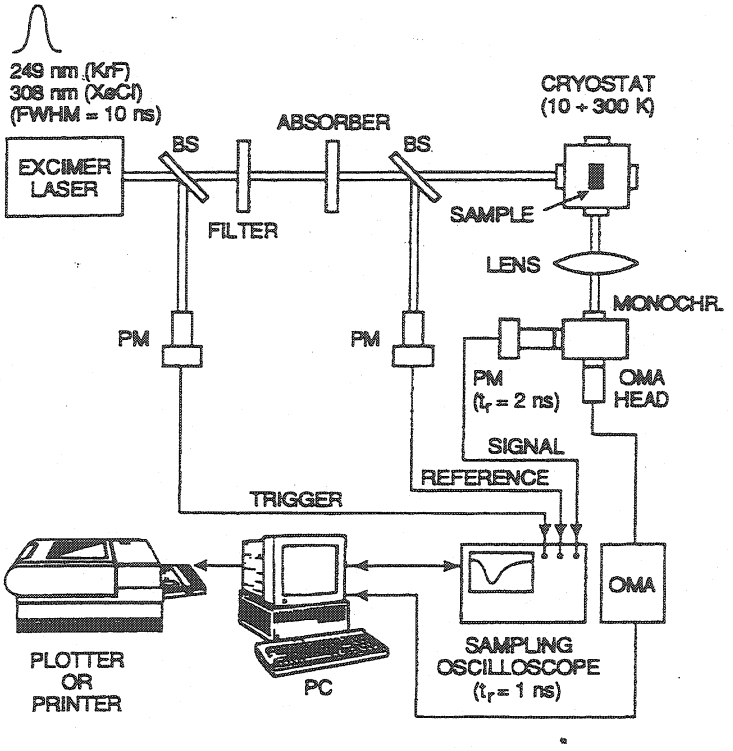

Figure 3: Experimental set-up for luminescence measurement (IFAC-CNR).

1.4 Neutron Radiography

The neutron tomography set-up is placed at the TRIGA thermal column and its scheme is reported in [5, 6]. A thermal flux of about $5*10^6$ $cm^{-2}s^{-1}$ is available at the exit of the radial thermal column when the reactor operates at its nominal power. The neutron beam passes through a collimator that can be circular, square or rectangular in section and has the shape of a truncated cone or pyramid. Nowadays the divergent-beam collimators are preferred to parallel-beam collimators to obtain the highest resolution. The ratio between collimator length L and its entrance aperture D (*collimator ratio*) influences also the presence of γ rays in the neutron beam, that could decrease the contrast of the radiographic image and hence the image resolution. The neutron flux increases much more rapidly with respect to γ rays as D increases, whereas both the fluxes (γ rays and neutrons) decrease when L increases. Consequently, the resolution improves with an increasing collimator ratio and with the use of gamma-ray filters.
The resolution of the radiograph is an important parameter and it is determined by several factors:
-the beam divergence, i. e. the ratio between the size of collimator inlet aperture and the distance between the inlet aperture and the point in the object to be analysed;
-the distance between the point in the object to be analysed and the image detection plane;
-converter thickness;

-distance between converter and imaging system.
In neutron radiographic applications direct and indirect imaging systems are used. The film-based image detection and recording techniques are classed as indirect because of an intermediate detector is used. The direct systems are represented by on-line or dynamic imaging detectors such as:
-planar detectors (e. g. low light TV cameras in combination with a fluorescent screen);
-line detectors (e. g. based on photo-multipliers arranged in line or photo-diodes detecting the light emitted from a scintillation and converter layer);
-point detectors (e. g. neutron detector tubes – BF_3, He_3 tubes – scintillator/photo-multiplier are under development).
Generally, the image detectors for neutron radiography provide a converter or intensifying function through the interaction with the incoming neutrons and the emission of a more directly detectable radiation like α, β or γ radiation. The resulting secondary radiation is monitored by recording it on photographic or nitrocellulose film, activation foils or by electronic detectors. Image detectors for direct or indirect image recording on film are made of metal foils of gadolinium, dysprosium, indium or gold and boron and lithium compounds coated on plastic foil.
The neutron tomography facility developed at the thermal column of TRIGA reactor concerns the imaging of industrial samples as well as the detection of hydrogen in metallic objects [5].
The TRIGA group acquired a good experience in the use of self-developed CCD (Charged Coupled Device) cameras and pioneered the use of back-illuminated sensors for neutron tomography applications. Tomographic projections are usually acquired with steps of 0.9° by using a turntable placed on a horizontal and vertical micrometric translation system that ensures an accurate centering of the detector. The system acquires 200 projections in about 30 min. The back projection reconstruction algorithm includes filters for the correction of spatial and temporal inhomogeneities of the neutron field. The software generates raw data sets that can be visualized with commercial tools and it is able to handle images from the cooled CCD presently in use (with a 192x165 pixel matrix) up to 512x512 pixels matrix. An intensifier for light from a NE426 scintillator with traditional optical coupling ensures the imaging with a typical acquisition time of about 55/frame.

CHAPTER 2: RESULTS AND DISCUSSION

2.1 Barium enriched glasses

Glass samples were submitted to γ irradiation at the "Calliope" ^{60}Co radioisotope source (ENEA-Casaccia, Rome) at the doses of 1 Gy, 3 Gy, 10 Gy, 50 Gy and 194.5 Gy with a dose rate of 3.6 Gy/h (in air). Before and after each irradiation, samples underwent transmission measurements performed by a double ray Perkin Elmer spectrophotometer. In Figure 4 the initial transmission spectra of all analysed glasses are reported. As it can be seen, they show the typical terbium absorption bands extending from 320 nm to 380 nm and peaking around 480 nm. These bands are due to the terbium electronic transitions $^7F_6 \rightarrow {}^5D_3$. As far as Ce^{3+} doped glass (sample TK8) is concerned, Ce^{3+} ion shifts the band edge position at higher wavelength (410 nm) because it introduces in the glass matrix absorption bands with a lower energy gap with respect to terbium.

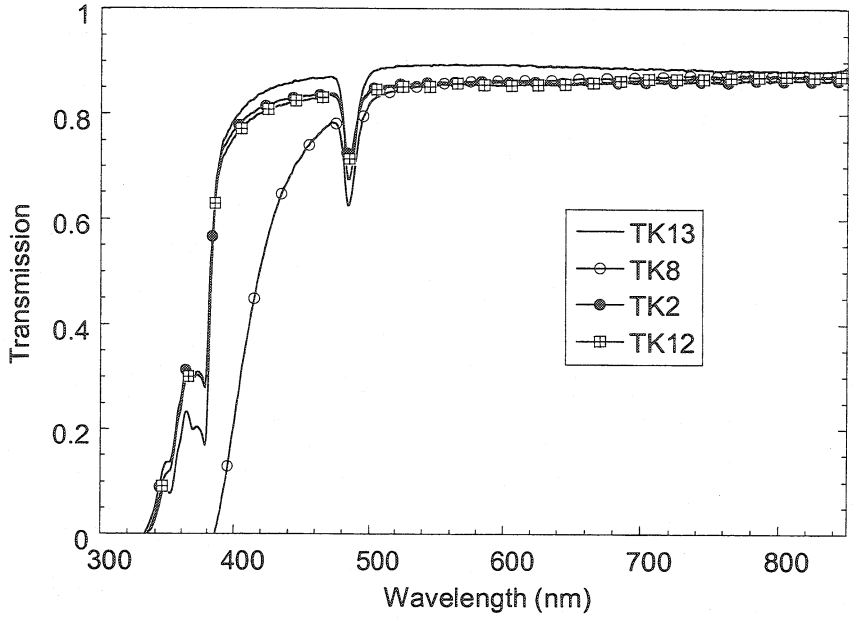

Figure 4: Initial transmission of all barium enriched samples

The γ irradiation of samples induces a transmission decrease higher at increasing doses, as reported in Figure 5 for TK13 glass.

To evaluate the density of colour centres induced by irradiation we calculated for all glasses the radiation induced absorption coefficient (μ), reported in Figure 6 for TK13 glass: as it can be seen, μ monotonically decreases with wavelength for all analysed samples and it becomes higher as the dose grows up. By comparing μ of all glasses, it is evident that the damage level depends strongly on the glass composition (Figure 7).

The only exception is represented by glasses TK13 and TK12 containing different terbium concentrations (4.2 and 2.7 mol %) and characterised by μ values practically identical at all wavelengths. This result agrees with a previous work of us [7] related to phosphate glassy matrices: analysing the radiation damage of phosphate glassy matrices containing different terbium content, it turned out that their radiation induced response was the same in the $TbPO_4$ concentration range 3-10 mol %. The observed results suggest that both in phosphate matrices and in silicate glass systems containing barium, the effect of irradiation is not very sensitive to changes of terbium concentration within the whole studied range. Cerium presence (0.5 mol %) in sample TK8 strongly improves (Figure 7) the radiation hardness of about 50 % (at 390 nm) with respect to the reference matrix with only terbium (TK13). The μ value is practically zero at

wavelengths higher that 548 nm. Till now similar results are carried out only in Heavy Metal Oxide glass matrices [8].

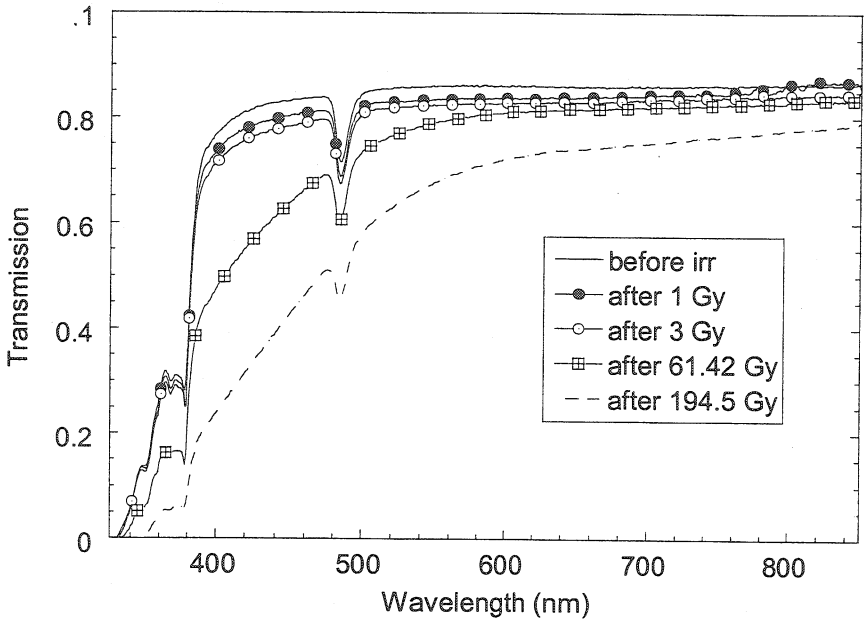

Figure 5: Transmission curves of TK13 glass after the various irradiation doses.

The Gd^{3+} and Tb^{3+} doped glass TK2 is less resistant to radiation with respect to glass containing only Tb^{3+} (TK12). In fact, the gadolinium content of 0.8 mol % negatively influenced the glass radiation resistance of about 20% at all the analysed wavelengths. At present there is not anymore paper which describes this effect related to gadolinium ions; hence, further investigation is required before making any kind of conclusion.

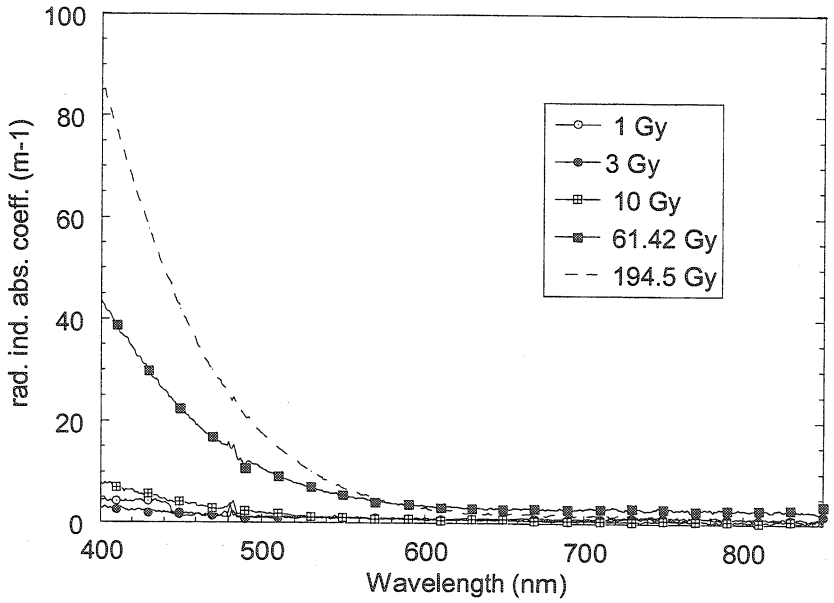

Figure 6: μ of TK3 glass calculated at different absorbed doses.

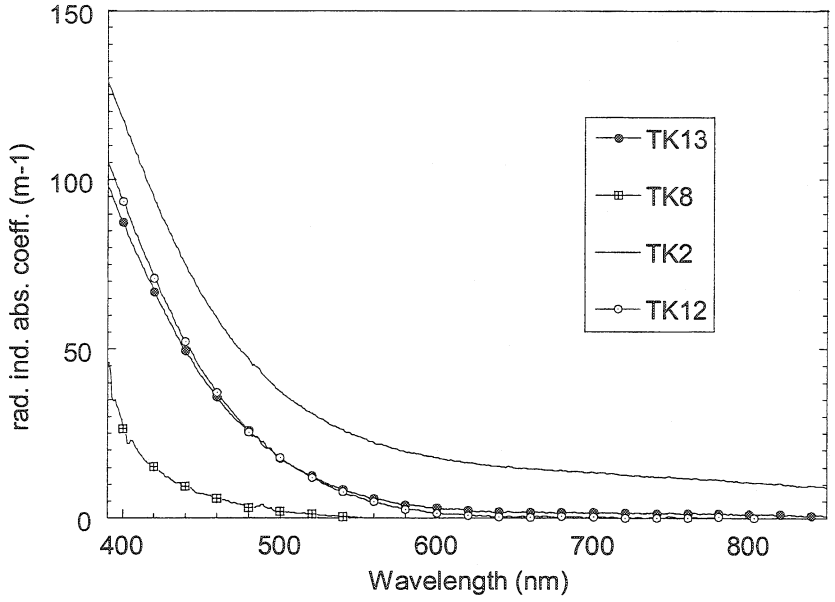

Figure 7: μ comparison of all glasses calculated at 194.5 Gy absorbed dose.

From the application point of view the wavelength of interest at which to analyse the glass radiation hardness is the one at which terbium emits its energy greatest part (542.5 nm). For this reason, in Figure 8, we reported the μ value at this wavelength. Results confirm that, from the radiation hardness point of view, the worst glass is the gadolinium doped one (TK2), which possesses a μ value linear with the dose. In samples TK13 and TK12 the damage saturates around 60 Gy and the cerium containing glass TK8 shows a μ value that, in the limit of experimental errors, is zero at all investigated doses.

The obtained results confirm the ability of cerium and terbium to make glass matrices resistant to irradiation, as it was already observed by other authors in previous works [9, 10, 11, 12, 13, 14, 15]. To explain such effect, it has to be reminded that in glass systems, the radiation induced bands absorbing light in the visible region are caused by hole centres (HC) entrapped in pre-existing defects (such as non bridging oxygen). If the irradiated glass matrix is doped with ions able to undergo radiation induced redox reaction processes, the distribution of the radiation induced colour centres is different from that of the undoped glass [16]. In particular, if the doping ions tend to acquire electrons, they serve as electron precursors; on the contrary, if their tendency is to lose the electron, they act as hole precursors. The consequence is that, when glass undergoes ionising irradiation, a kind of competitive process is primed between intrinsic and extrinsic electron/hole precursors in the capture of charge carriers moved by radiation. In our case, this seems to be the most plausible explanation for the analysed samples since $Ce^{3+}$and Tb^{3+} ions are characterised by such valence electron configurations for which they tend to lose an electron in accordance with the following radiation induced redox-reaction [17, 18]:

$$X^{3+} + \gamma \Rightarrow (X^{3+})^{+} + EC \qquad (2.1)$$

In this sense they act as hole precursors by capturing holes produced in the process of irradiation and lowering the absorption related to HC existing in the glass network.

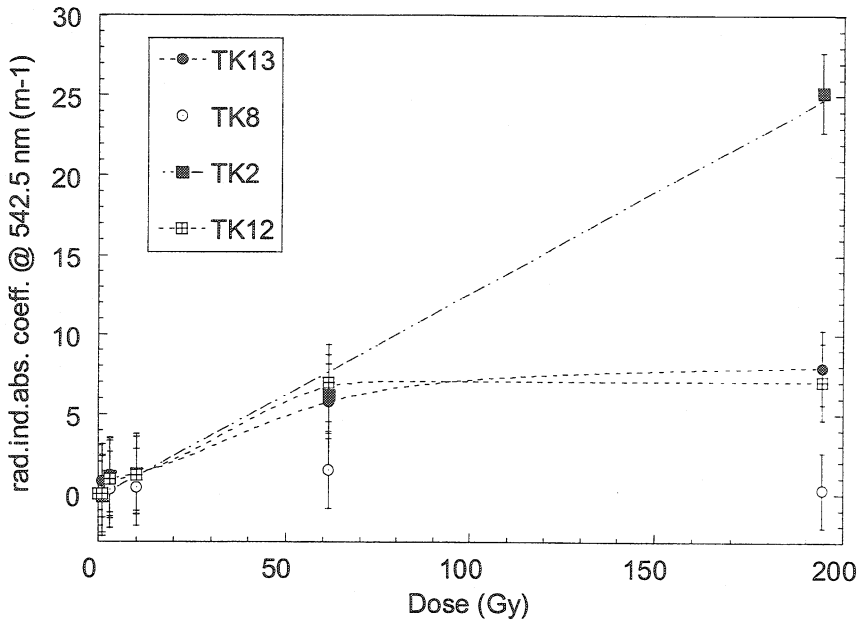

Figure 8: μ @ 542.5 nm for all glasses at the different irradiation doses.

As far as the decay kinetic is concerned, samples TK12 and TK13 are characterised by a slow emission component (≈10 ms). Besides the typical terbium related peaks, the TK12 glass emission spectrum shows also a broad band around 430 nm, probably related to the presence of a defect in the silicate glass (Figure 9) .

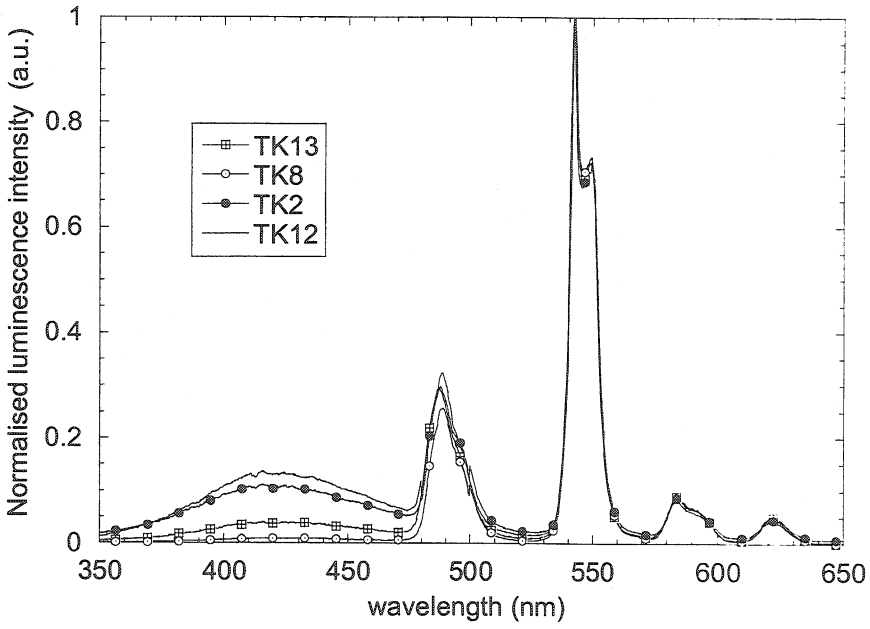

Figure 9: Normalised Emission spectra of samples TK2, TK8, TK12, TK13.

Matrix defects favour the energy transfer from the glass matrix to terbium luminescent centres, which decay slowly. For this reason, the sample TK12 decay is much slower than TK13 one; in fact, the emission spectrum of TK13 sample shows a smaller band around 430 nm, i. e. matrix defects are fewer than in TK12 glass. The decay curve can be fitted by means of two exponential components of about 40-50 ns and 300-320 ns decay times with the dominant contribution of the latter one (Figure 10).

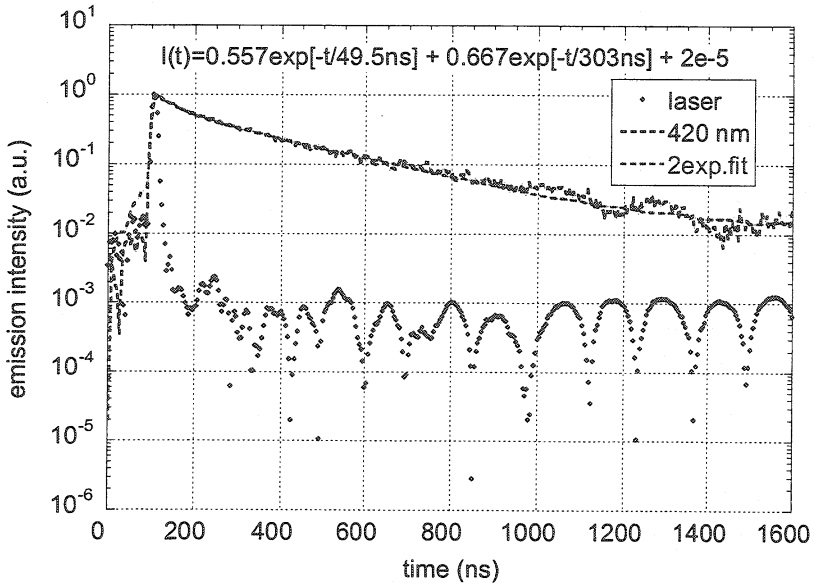

Figure 10: Decay curve sample TK12; Exc=308 nm (XeCl-laser), Emis.=420 nm, room temperature.

To explain this kinetics, two hypothesis are plausible:
- there are two closely spaced excited levels, each characterised by its own decay time, so that the curve shows the sum of both the decay processes;
- there is some kind of energy transfer from the excited state to some matrix centre, which distorts the decay exponential behaviour and this distortion can be fitted by means of two exponential.

In the sample TK2 the presence of gadolinium does not change decay time in a meaningful way respect to TK12 and also the matrix excitation is similar (emission band around 430 nm). In the sample TK8, the presence of cerium centres introduces also a fast component (about 40-50 ns) in the decay kinetic (Figure 11).

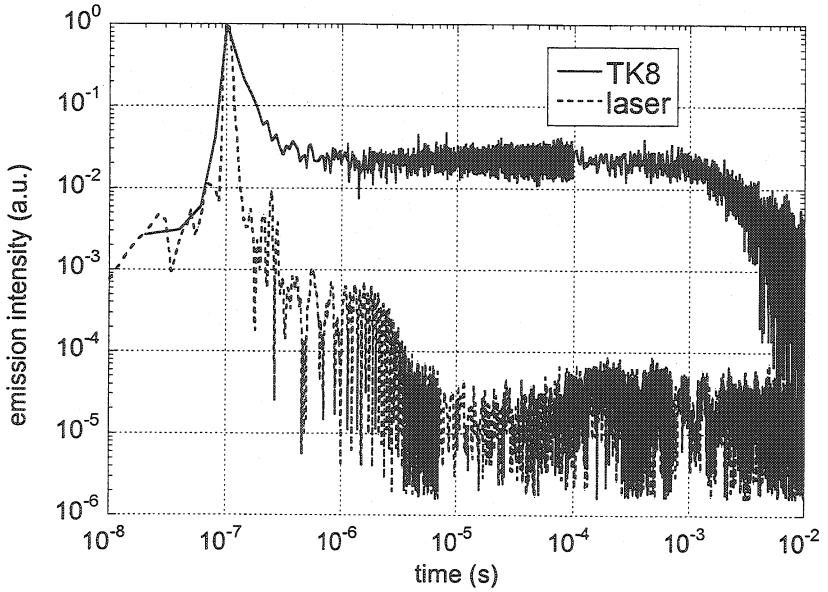

Figure 11: Decay curve sample TK8; Exc=308 nm (XeCl-laser), Emis.=545 nm, Room Temperature.

This effect can be explained considering that cerium reduces energy transfer to terbium ions because its effect prevails on the effect of matrix defects. In fact, as a consequence

of cerium presence in the sample there is the reduction of the emission band around 430 nm.

2.2 Boron enriched glasses

As far as the neutron radiography is concerned, it was performed by using two samples (BK10 and BK11) characterised by the same glass composition of samples TK12 and TK13 with an additional content of boron, because of its high absorption cross section for thermal neutrons. Specifically, ^{10}B upon absorbing a neutron almost immediately is transformed in ^{11}B. The latter rapidly decays to produce, among other particles, ninety-four 0.478 MeV gamma-rays per 100 ^{10}B neutron absorption.
The nuclear reaction is the following:

$$^{10}_{5}B + n \rightarrow {}^{11}_{5}B \rightarrow {}^{7}_{3}Li^{*} + \alpha \qquad (2.2)$$

$$^{7}_{3}Li^{*} \rightarrow {}^{7}_{3}Li + \gamma \qquad (2.3)$$

The γ-rays produced in this reaction excite the glass matrix luminescence centres and the scintillation light is collected by the CCD camera. The images are obtained from a set of projections, recorded with a 30 s acquisition time. Then we reconstructed the image by a mathematical algorithm. During acquisition scan, samples are located nearby in the experimental set-up and consequently they are reported together in each image (BK10 on the right and BK11 on the left part of the figure respectively).

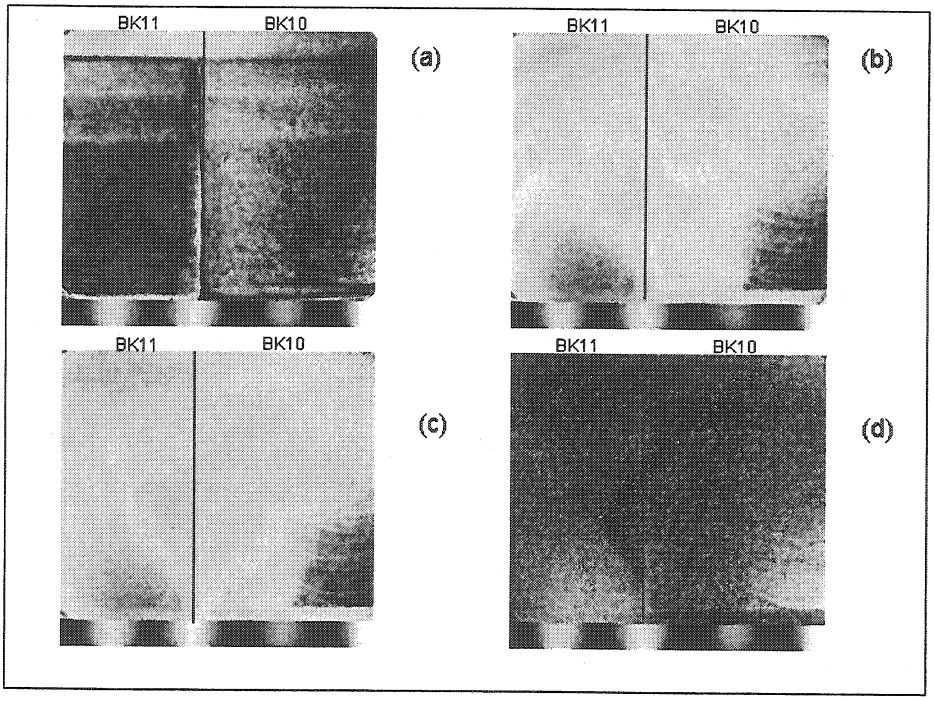

FIGURE 12: Radiography of samples BK10 and BK11 immediately after neutron irradiation (a), after 2 minutes (b), after 60 minutes (c) and after 1 day (d).

The scintillation light was measured in arbitrary units using the colour scale below each figures. In spite of the different glasses thickness there is no difference between the two samples in the scintillation light intensity. The highest emission is localised on the borders of the glasses. Another interesting result is that samples are characterized by a phosphorescent component: after the maximum emission (violet in the colour scale

corresponding to 30% of the maximum light recordable by CCD camera) measured immediately after the irradiation, samples still emitted light.
In order to get information about the lifetime of this phosphorescent component, we repeated measurements after 2 (Figure 12a), 5(Figure 12b) and 60 minutes (Figure 12c) and after one day (Figure 12d) from the stop of irradiation: as it can be seen from the figures above, light is emitted in a non homogeneous way by each sample and there is practically no difference between the image recorded after 2 minutes and 1 hour. On the contrary, after one day the light intensity decreases of about 50 % respect to the first acquisition.
In order to get information about the activators responsible for the phosphorescent component, using the experimental set-up described in section 1.3.b we studied the emission spectra of BK10 and BK11 samples at two different excitation length (310 nm and 380 nm). The result is reported in Figure 13 and shows that BK10 and BK11 samples have the same activators of Ba-rich glasses examined in previous pages. In fact, we can note the typical emission peaks of terbium at 482, 545, 585 and 621 nm. Moreover we note also a band around 370 nm, that like the band around 430 nm of Ba-rich glasses is due to matrix excitation.
On the basis of the observed results it turns out that the examined glasses are not suitable to be used in a neutron tomographic system, in which the acquisition rate requires the absence of any phosphorescence component.

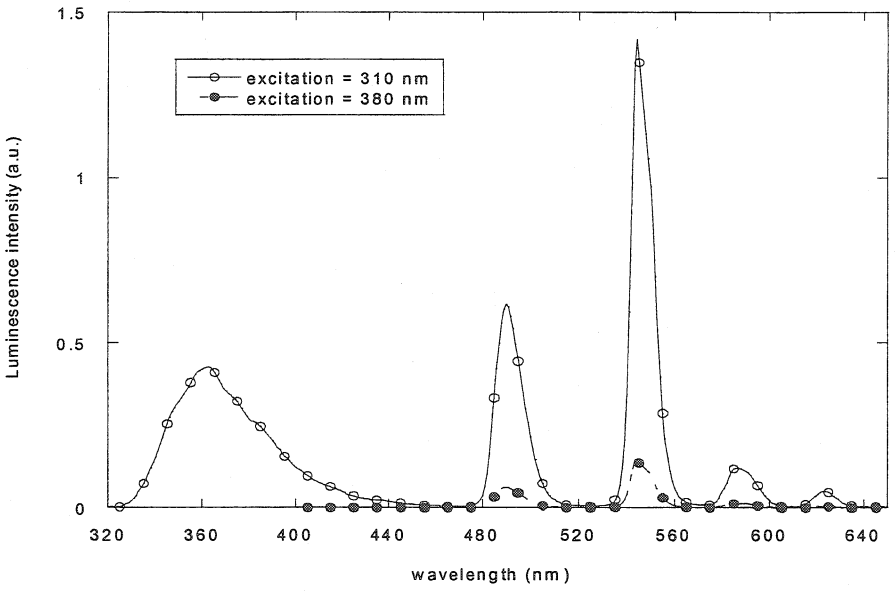

Figure 13: Emission spectra of BK10 and BK11 samples.

CONCLUSIONS

The effect of ionising radiation on trivalent rare earth doped Ba-rich glasses is similar and the damage level is much lower than undoped matrix glasses. A possible explanation for the observed result could be a kind of competitive process between doped trivalent rare earth ions and intrinsic glass hole precursors in the capture of the holes moved by irradiation. Rare earth ions are probably more efficient than intrinsic hole precursors in capture holes, and it implies a reduction of the visible absorption bands related to intrinsic hole centers.

Moreover the results obtained by neutron radiography showed that it is impossible to use the examined boron-rich glasses for a neutron tomography because of their phosphorescence still alive one day after the irradiation. In fact, tomographic technique is based on repeated image acquisitions, and the scintillating glass should be completely de-excited before the next scan.

From this analysis some aims for a future research emerge: the study of the role of matrix defects (in particular related to oxygen) in the Ba-rich and B-rich glasses by means of annealing in vacuum and in air, and the investigation about the possibility to dope B-glasses with fast activators (i. e. cerium) for a neutron tomographic system.

Acknowledgements
The authors are grateful to Mr. Angelo Pasquali and Mr. Francesco Zarbo for their technical support in irradiation tests (Calliope Facility); Prof. Franco Casali (Physics Department of University of Bologna), who provided the samples from the "Vavilov" State Optical Institute of Saint Petersburg (Russia); Dr. Martin Nikl (Academic Science of Prague) for scientific discussion.

References

1. BETTINELLI M., INGLETTO G., POLATO P., POZZA G., ZANELLA G., ZANNONI R., "Optical spectroscopy of Ce^{3+}, Tb^{3+} and Eu^{3+} in new scintillatine glasses", Phys. Chem. Glasses 37 (1), pp. 4-8, 1996.

2. RODNY P. A., *"Physical Processes in inorganic scintillators"*, CRC Press, New York, 1997.

3. BACCARO S., FESTINESI A., BORGIA B., "Gamma and neutron irradiation facilities at ENEA-Casaccia Center (Rome)", Cern-CMS Technical Note 1995/192.

4. ADAMO M., BACCARO S., CECILIA A., CEMMI A., PASQUALI A., ZARBO F., "Metodi dosimetrici presso l'impianto di irraggiamento Calliope", ENEA Rapporto Tecnico ENEA-INN/2000/3.

5. ROSA R., BEDOGNI R., BURGIO N., GUALDRINI G., TORTORELLA D., "Neutron and photon experimental characterization for an improved neutron radiography facility at ENEA Casaccia Triga reactor" *7th World Conference on Neutron Radiography*, Rome (Italy), 15-20 September 2002.

6. ROSA R., FESTINESI A., MASSARI, SANGIOVANNI R.G., SANTORO E., STORELLI L., "A tomography system at the thermal neutron column of the ENEA Casaccia TRIGA reactor", Appl. Phys. A 74 [Suppl.], S1683-S1685, 2002.

7. BACCARO S., CECILIA A., CEMMI A., CHEN G., MIHOKOVA E., NIKL M., "Optical characterisation under irradiation of Ce^{3+}(Tb^{3+})-doped phosphate scintillating glasses", IEEE Transaction on Nuclear Sciences, Volume 48, number 3, 2001.

8. BACCARO S., CECILIA A., CHEN G., DU Y., M. MONTECCHI, WANG H., WANG S., "Effects of irradiation on transmittance of cerium doped germanate in the ultraviolet and visible regions", NIM B, 191, pp. 352-355, 2002.

9. WEBER M.J., "Heavy Scintillators for scientific and industrial applications", Proceedings of the CRYSTAL 2000 International Workshop, edited by F. De Notaristefani, P. Lecoq, M. Schneegans, Chamonix (France), Sept. 1992.

10. BACCARO S., CECILIA A., MONTECCHI M., NIKL M., POLATO P., POZZA G., ZANELLA G., ZANNONI R., "Radiation damage of silicate glasses doped with Tb^{3+} and Eu^{3+}", J. Non-Crystalline Solids, 315/3, 271-275, 2003.

11. BACCARO S., CECILIA A., CHEN G., DU Y., E. MIHOKOVA E., NIKL M., NITSCH K., "How cerium affects irradiation resistance", *American Ceramic Society Bullettin*, Vol. 80, n° 4, pp. 107-110, 2001.

12. BACCARO S., CECILIA A., CHEN G., DU Y., MONTECCHI M., WANG H., WANG S., "Transmission properties of heavy germanate glasses as hosts for scintillating rare earth", *NIM A*, 486, pp. 321-324, 2002.

13. BACCARO S., CECILIA A., MIHOKOVA E., NIKL M., NITSCH K., POLATO P., G. ZANELLA G., ZANNONI R., "Radiation damage induced by gamma irradiation on cerium doped phosphate and silicate scintillating glasses ", *NIM A*, 476, pp. 785-789, 2002.

14. BACCARO S., CECILIA A., CEMMI A., E. MIHOKOVA E., NIKL M., NITSCH K., POLATO P., G. ZANELLA G., ZANNONI R., "Colour centres induced by gamma irradiation in scintillating glassy matrices for middle and low energy physics experiments", NIMB 185/1-4, 294-298, 2001.

15. BACCARO S., et al., "Development of scintillators based on glassy matrices - Newlumen experiment", *Report N. 1120 INFN/Dip. Fisica*, 2002.

16. EHRT D., VOGEL W., "Radiation hardness in the glasses", *NIM B, 65*, pp. 1-8, 1992.

17. EBENDORFF- HEIDEPRIEM H., EHRT D., "Formation and UV absorption of cerium, europium and terbium ions in different valencies in glasses", Optical Materials; 15, pp. 7-25, 2000.

18. ARBUZOV V.I., Journal of Non Crystalline Solids **253**, pp. 37-49, 1999.

Edito dall' ENEA
Funzione Centrale Relazioni Esterne
Unità Comunicazione
Lungotevere Thaon di Revel, 76 - 00196 Roma
www.enea.it
Stampa: Laboratorio Tecnografico ENEA - CR Frascati
Finito di stampare nel mese di luglio 2003